UNIVERSITY OF GRONINGEN

The steam methane reforming reaction in a plug-flow reactor simulated

Investigating the steam methane reforming reaction efficiency dependency on the mass flow rate of the gas in a plug-flow reactor with an uneven temperature profile.

Authors:
Djano PERSOON *(s4853830)*

First Supervisor:
DR. ANATOLI V. MOKHOV
Second Supervisor:
PROF. DR. ARAVIND PURUSHOTHAMAN VELLAYANI
Daily Supervisor:
YANG LI

Bachelor's Thesis
To fulfill the requirements for the degree of
Bachelor of Science in Physics
at the University of Groningen

July 4, 2024

Contents

1 Abstract

In the investigation set out in this thesis, the steam methane reforming reaction in a plug-flow reactor was investigated through the use of computational methods. The goal of this investigation is to examine the dependence of the efficiency of an ideal reactor with an uneven temperature profile on the mass flow rate of the gas.

For the simulations, the "gri30.yaml" reaction mechanism and the Cantera package in Python have been used. First, an ideal zero-dimensional constant-pressure reactor was simulated to evaluate the temperature dependency of the hydrogen production rate.

Afterwards, using the temperature profile of real experimental data, a temperature fit using an error function was made, after which its upper limit was offset to realize a higher maximum temperature. This fit was used as the temperature profile of an external heat reservoir. This reservoir was connected to a plug-flow reactor using Cantera's wall object, allowing heat transfer. Then the gas temperature, time step per unit length, hydrogen mole fraction and hydrogen production efficiency were plotted against the length of the reactor for a variety of mass flow rates.

For the plug-flow reactor, it was observed that the deviation between the gas temperature and reservoir temperature increased as the mass flow rates increased. Both the lower temperature and decreased residence times resulted in an observed lower hydrogen mole fraction and lower production efficiency for higher mass flow rates.

Keywords: Steam methane reforming, plug-flow, chemical kinetics, heat transfer

2 Acknowledgment

I want to thank my supervisor, Dr. Anatoli V. Mokhov, for his insights and advices. I also used the kinetics package in Python, which he developed, to evaluate the validity of my results. I did not meet him often, but when I did, his insights were invaluable. The scope of my investigation was essentially reshaped in a way that made my research significantly more valuable within the field of combustion physics. In addition, his advice will help me in my future career as a researcher.

I also want to express my gratitude for my daily supervisor, Yang Li. He introduced me to relevant literature and the Cantera package. Moreover, he provided fundamental pieces of codes I could use for my simulations and he has helped me debugging and verifying the validity of my results. He was a major influence for my theory section, as he introduced and explained the governing equations within chemical kinetics and plug-flow in detail to me. I mentioned earlier that I did not meet with Dr. Anatoli often, but this is because Yang had regular meetings with Dr. Anatoli to discuss how he could best guide me and my learning process. Moreover, I want to thank Yang for his readiness to help out, and his fast responses when I contacted him with questions. I also want to thank him for his time, his patience with me, and his dedication.

3 Introduction

In December 2015, the United Nations gathered to hold the 21st Conference of Parties in Paris [1]. The purpose of this conference was to address the accelerated global warming caused by human activities. This resulted in the Paris Agreement, which states that the global temperature increase must be limited well below 2 degrees Celsius by the end of the 21st century compared to preindustrial levels [1]. In order to achieve this goal, countries worldwide have to reduce their greenhouse gas emissions. The main greenhouse gases are produced and released into the atmosphere when burning oil, gas, and coal, or through intensive livestock farming [1]. Hydrogen in the contrary, produces no greenhouse gases upon burning [2] [3]. In this perspective hydrogen could therefore be a good alternative compared to fossil fuels.

The steam methane reforming (SMR) reaction process is a mature hydrogen production process and is likely the most cost-effective large-scale hydrogen production method for the foreseeable future [4]. The SMR reaction is an endothermic reaction that converts methane and water into hydrogen and some by-products [5]. After the SMR reaction has occurred, impurities can be removed from the gas stream in a final process so that essentially only hydrogen will be left in the final gas stream [5]. This hydrogen can then be used in hydrogen-powered fuel cell vehicles, to produce ammonia for fertilizers, to replace natural gas in iron and steel production in industry, and for a variety of other chemical production and industrial processes [4].

The hydrogen produced through the SMR reaction thus has a variety of applications, and therefore it is clear that the SMR has an important role for the current and future industries and transport. As for this research and development are investigating methods and refining steam reforming reactor designs to increase efficiencies even further [4]. For this experimentation is required. As mentioned earlier, the SMR reaction is endothermic and thus temperature dependent. As for this temperature sensitivity, it is preferred that an environment with a precise temperature can be created. A furnace is a commonly used instrument in chemical reaction research to achieve these desired constant temperatures. Schltinder defines a furnace as "an insulated chamber in which heat is transferred from a high-temperature source to a sink" [6].

Ideally, the temperature distribution of the furnace is stable, even, and precise. However, due to manufacturing issues and heat exchange with surroundings, the temperature distribution always deviates from the ideal situation [6]. Before conducting an experiment, one should have identified the exact temperature profile of the furnace.

Computer simulations can contribute to the progress within both fields of chemistry and physics. Simulations can predict outcomes of experiments. New reactor designs can be simulated after which data can be obtained, and limitations of a design can be identified before actually building these reactors for example. Afterwards sophisticated experiments have to be conducted to verify the results of the simulations. If the results obtained from the experiment do not align with the simulations, then the mathematical models behind the simulations should be updated. [7]

In the investigation set out in this thesis, the steam reforming reaction of methane will be investigated through the use of computational methods. The goal of this investigation is to examine the dependence of the SMR hydrogen production, in terms of the hydrogen mole fraction and production efficiency, on the mass flow rate of the gas in an ideal plug-flow reactor with an uneven temperature profile.

4 Theory

The computational methods behind the simulations make use of several calculations. These calculations are a necessity to predict species distributions, flow and gas temperature profiles along the reactor length. The equations set out in this section are fundamental for understanding the physics behind the simulated chemical flow reactor.

4.1 Chemical kinetic calculations

Chemical kinetics is about the study of the rate of chemical reactions. The reaction rate is the concentration change of reactants and products per unit of time [7]. When considering an elementary reversible chemical reaction, one can represent the reaction in the general form [8];

$$\sum_{k=1}^{K} v'_{ki} X_k \rightleftharpoons \sum_{k=1}^{K} v''_{ki} X_k \ (i = 1,...,I), \tag{1}$$

where the subscript k represents the kth species in the reaction, X the chemical symbol, v' the stoichiometric numbers corresponding to the reactants and v'' corresponding to the products. The stoichiometric numbers represent the mole fractions of the species in the reaction.

However, often a variety of different elementary reactions occur in real reactors. The rate-of-progress variable (q_i) for each individual reaction denoted by subscript i, is equal to the reaction rate of each individual reaction and can be described as [8];

$$q_i = k_{f_i} \prod_{k=1}^{K} [X_k]^{v'_{ki}} - k_{r_i} \prod_{k=1}^{K} [X_k]^{v''_{ki}}, \tag{2}$$

where k_f and k_r are the forward and reverse rate coefficients respectively, and $[X]$ is the molar concentration. It can be noted that the stoichiometric numbers also represent the reaction orders when considering the reaction rates. However, as species X can both play a role in the forward and the reverse reaction, the net stoichiometric number of the kth species can be written as [8];

$$v_{ki} = v''_{ki} - v'_{ki} \tag{3}$$

Using the net stoichiometric numbers and the rate-of-progress variables the net molar production rate ($\dot{\omega}_k$) can be calculated [8];

$$\dot{\omega}_k = \sum_{i=1}^{I} v_{ki} q_i \ (k = 1,...,K), \tag{4}$$

4.2 Plug-flow calculations

The plug-flow reactor model is a mathematical approximation to real life laboratory reactors regularly used in the field of chemical kinetic studies [9]. It is a relatively simple model that considers an one-dimensional flow through an ideal reactor. Despite this, it can be used to model complex practical situations [9]. The model relevant to this Thesis considers a cylindrical channel with a fixed cross-sectional area. The plug-flow approximation is more accurate when used to model reactions at higher temperatures (temperatures higher than 1000K) [9].

The plug-flow approximation assumes a steady and continuous flow. It is also assumed that there is no diffusive transport in the primary flow direction of the gas. Therefore, for every unit volume within the reactor, the amount of mass per unit time (the mass flow rate) must be conserved. The

simplified mass continuity equation of the flow in the reactor was derived by Kee et al. [9] and can be described as;

$$\frac{d(\rho u)}{dz} = 0, \tag{5}$$

where z is the axial position, ρ the gas density, and u the flow velocity. However, in the cross-stream direction, strong mixing does occur [9]. When the mass flow rate, gas composition and pressure (P) of the system are known, one can use Eq. 5 to calculate the flow velocity of the gas. The gas density can be calculated using the ideal gas law [9];

$$P = \frac{\rho RT}{\overline{W}}, \tag{6}$$

where R is the ideal gas constant, $\overline{W}$ is the mean molecular weight, and T is the gas temperature. The gas temperature (T) can be calculated when the wall temperature (T_w) is known, considering that the energy within a system must be conserved. The plug-flow energy equation as derived by Kee et al. [9];

$$\rho u c_p \frac{dT}{dz} = \frac{\hat{h}P}{A_c}(T_w - T) - \sum_{k=1}^{K} h_k(\dot{\omega}_k W_k) \tag{7}$$

where c_p is the mass-averaged mean specific heat capacity of the gas at constant pressure, $\hat{h}$ is the heat-transfer coefficient, P the channel perimeter, A_c the cross-sectional area, h the specific enthalpy, and W the molecular mass. The heat-transfer coefficient can be calculated directly using the Nusselt number (Nu) [10];

$$\hat{h} = Nu\frac{k}{D}, \tag{8}$$

where D is the channel's inner diameter, and k is the thermal conductivity of the gas.

Nusselt number depends on both Reynolds number (Re) and Prandtl number (Pr) through Graetz number (Gz) [10];

$$Gz = \frac{RePrD}{z}, \tag{9}$$

with;

$$Pr = \frac{c_p\mu}{k}, \tag{10}$$

and;

$$Re = \frac{\rho uD}{\mu}, \tag{11}$$

where μ is the viscosity of the gas.

Often Reynolds number is used to determine if laminar flow ($Re < 2100$) or turbulent flow (very large Reynolds number) is more appropriate to use as an approximation [10]. When assuming laminar flow and a constant wall temperature, Nusselt number can be described as [10];

$$Nu = \begin{cases} 3.657 + 0.2362Gz^{0.488}e^{-\frac{57.2}{Gz}} & \text{for } Gz \leq 1000 \\ 1.077Gz^{\frac{1}{3}} - 0.7 & \text{for } Gz > 1000 \end{cases}, \tag{12}$$

Species and temperature might vary along the channel's length. However it is assumed that there is no variation across the channel. Because of this and the steady-flow assumption, one can derive the species conservation equation as has been done again by Kee et al. [9];

$$\frac{d(\rho Y_k u)}{dz} = \dot{\omega}_k W_k, \tag{13}$$

where Y is the mass fraction.

5 Methods

For this investigation multiple steam methane reforming reactions were simulated in Python using the Cantera package [11]. All simulations used an ideal gas reactor with either constant pressure or near-constant pressure. The reaction mechanism used for the simulations is "gri30.yaml" [12]. The simulations simulated natural gas combustion without the use of a catalyst. The internal pressure was set to be equal to 1 atmosphere. The initial methane-to-water mixing ratio in the gas sample was set to be 1:2 to avoid solid carbon formation based on the results of chemical equilibrium calculations. The developed codes have been uploaded to Github and can be accessed using the following link: Simulation code

5.1 Zero-dimensional reactor model

The first set of simulations served as "ideal" cases, as the modeled reactor was zero-dimensional and did not consider mass flow through the system. For these simulations, the conservation of energy had been neglected. This choice had been made because otherwise the temperature within the reactor would decrease as a result of the endothermic nature of the SMR reaction. The step size of the simulation was set to be 10000. After 10000 steps, the accuracy is not so sensitive to the number of steps according to a performed test. The hydrogen mole fraction had been plotted against time for a set of constant temperatures between 800 K and 1600 K. The reaction rates were expected to be faster for higher temperatures because of the endothermic nature of the reaction.

5.2 Plug-flow reactor model

To simulate a plug-flow reactor, the so called "Chain of Reactors Simulation model" has been used. In this model, the gas flows through multiple stationary volumes. The volume lengths were determined by the chosen step size. If an infinite number of steps would be chosen, the volumes would be of an infinite small length, effectively simplifying the one-dimensional plug-flow reactor into a series of zero-dimensional reactors. For these simulations a step size of 10000 was chosen. The gas composition and properties of the first reactor in this chain were defined using manually installed parameters and calculations made by Cantera [11]. The inlet composition of the downstream reactor would then be equal to the composition of the directly adjacent upstream reactor. As the flow in an ideal plug-flow reactor is steady, there is no diffusion inside the reactor. Therefore none of the upstream reactors was affected by any of the downstream reactors. For this it was possible to integrate every reactor to steady state, while going from the first to the last reactor in the chain.

For this simulation the same volumetric flow rate ($1.86 \cdot 10^{-4}$ m s^{-1}, at standard conditions) and reactor dimensions ($r = 6$ mm) as Kahle et al. was used [13]. The volumetric flow rate has been used to calculate the mass flow rate ($\dot{m}$) using the ideal gas law equation (Eq. 6). A pressure gradient of 10^{-5} was used for simulation technicalities. An initial gas temperature of 400 Kelvin was used to ensure that all water vapour would be in the gaseous state. Example codes were provided by Cantera [11]. These were modified to implement energy conservation within the system and heat transfer from an external reservoir to the gas, making the simulation more accurate to a real reactor. A wall object was used to connect the reservoir to the reactor tube. The wall temperature at each position was constant over time. It was assumed that there was only convective heat transfer between the gas and the wall, thus the overall heat-transfer coefficient of the wall could directly be calculated using Eq. 8 . Temperature data of Kahle et al. was used to have the reservoir temperature match the uneven temperature profile of a real furnace [13]. A fit was made to the temperature data points of three different temperature profiles. The average of the parameters of these three fits were taken to create a new, more accurate fit. The upper bound of this fit was then offset with 350 Kelvin in order to

simulate a furnace with a higher temperature than Kahle et al.'s furnace. The temperature profile as defined by the fit was of the form;

$$T = \begin{cases} erf(E(z-a))\frac{A}{2} + B + \frac{A}{2}, & \text{for } z \leq \frac{a+b}{2} \\ -erf(E(z-b))\frac{A}{2} + B + \frac{A}{2}, & \text{for } z \geq \frac{a+b}{2} \end{cases}, \tag{14}$$

where a, b, A, B and E are parameters. Using this temperature profile, a temperature was assigned to the reservoir for each intermediate step. For each step, the change in chemical composition was calculated using Cantera. With the changing composition the change in the flow velocity was calculated as well. The gas temperature, the time step per unit length (Δt), the hydrogen mole fraction and production efficiency were evaluated by plotting them against the length of the reactor for multiples of the mass flow rate of Kahle et al.

The hydrogen production efficiency was defined as follows;

$$\text{Efficiency} = \frac{\text{Realized mass fraction}}{\text{Theoretical mass fraction}} \cdot 100\% \tag{15}$$

The "Theoretical mass fraction" is assumed to be correctly represented by the following formula;

$$\text{Theoretical mass fraction} = \frac{4W_{\text{H}_2}}{W_{\text{CH4}} + 2W_{\text{H2O}}}, \tag{16}$$

Here it was assumed that all hydrogen atoms present in the initial gas, which was determined by the earlier mentioned methane-to-water mixing ratio, are available to form hydrogen molecules.

Assuming that $\overline{W}$ is almost constant for very small time steps and considering the near constant pressure differences per unit length, when the temperature increases, the density must decrease according to Eq. 6. As the density decreases, the flow rate must increase according to Eq. 5. Thus, it was expected that the time step per unit length decreases for higher temperatures. However it was expected that a higher temperature would still result in a higher SMR reaction efficiency. It was also expected that a higher mass flow rate would result in a lower efficiency as a result of shorter residence times, which effectively are the sum of time steps per unit of length over the entire length of the reactor.

5.3 Validation of the model

To validate the model, results obtained through the model were compared to experimental data of Kalhe et al. [13]. This test case did not consider heat transfer from an external reservoir but assumed that the gas was already at a temperature of 1123, 1173 or 1223 Kelvin. Furthermore the test case did not use the hydrogen mole fraction produced through the SMR reaction for comparison, but the methane and CO_2 conversions for an initial gas composition of CO2:0.425, CH4:0.425, H2:0.1, Ar:0.05. The test case was the same as the plug-flow reactor model in all other aspects. The methane and CO_2 conversions were then plotted against the temperature for both simulation and experimental data.

6 Results & Discussion

6.1 Zero-dimensional reactor simulation

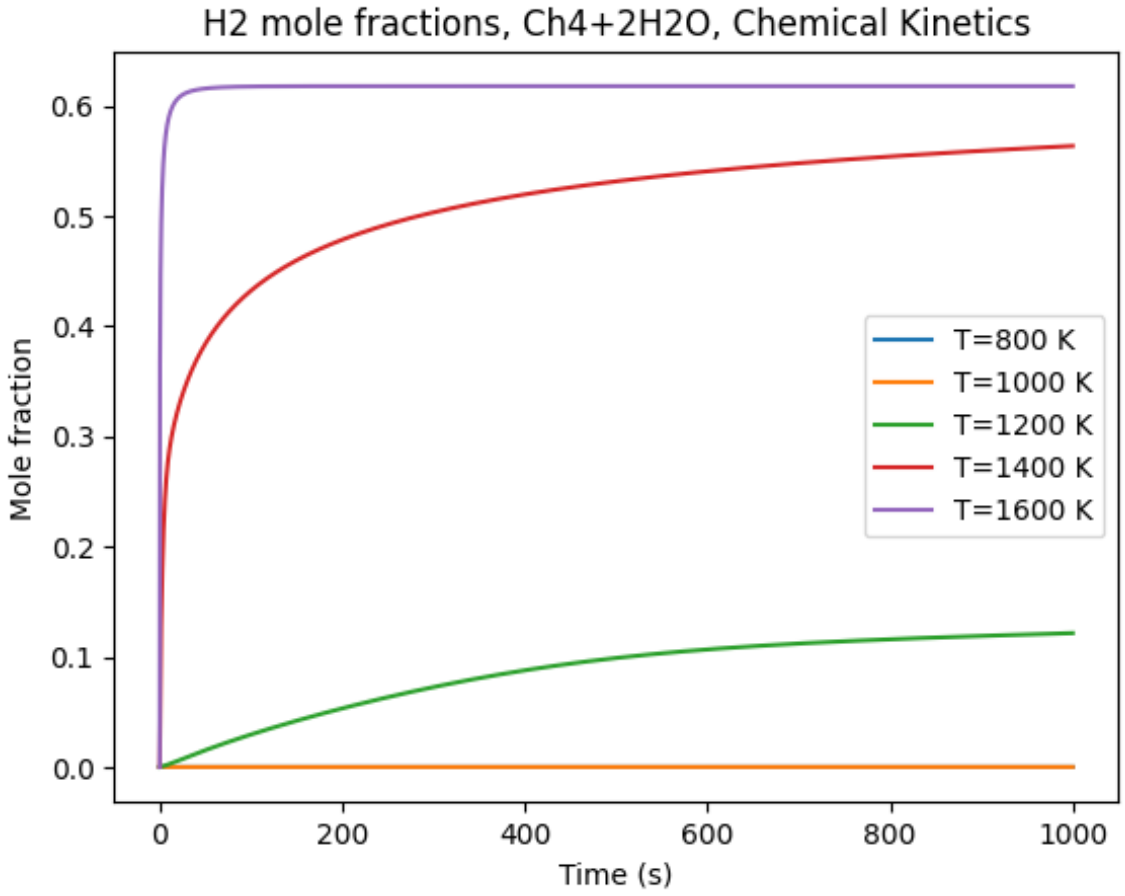

Figure 1: *The hydrogen mole fraction against the time in seconds for a set of different temperatures in Kelvin, for a gas inside zero-dimensional reactor.*

As can be seen in Figure 1 above, more H_2 is produced per unit time when the temperature is higher, resulting in a higher final H_2 concentration at t= 1000s for higher temperatures. For T=1600 K, most hydrogen production seems to occur during the first few seconds. After this initial hydrogen concentration increase, the hydrogen concentration seems to approach a horizontal asymptote. The time duration for when this asymptote seems to be reached seems to decrease for increasing temperature. These findings are in correspondence with the expectations mentioned in the Methods section.

6.2 Plug-flow reactor simulation

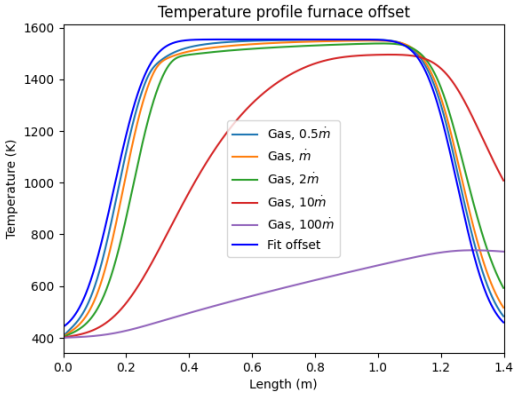

(a) *The offset temperature fit and the temperature of the gas.*

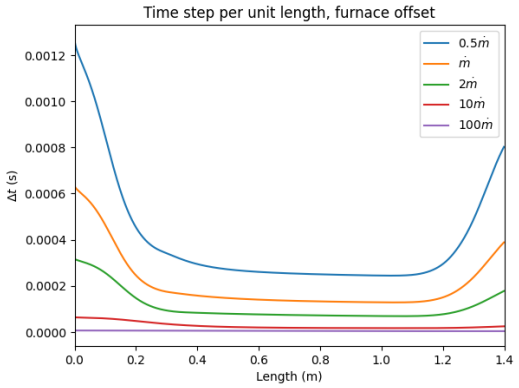

(b) *Time step per unit length.*

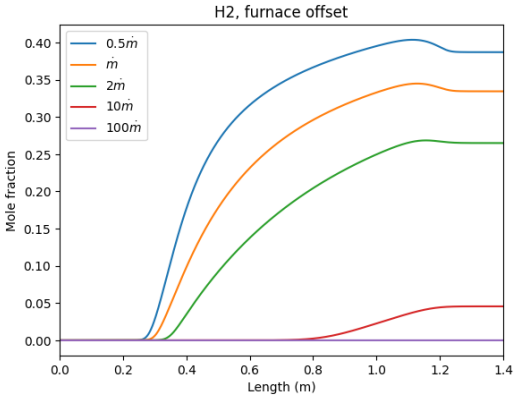

(c) *Hydrogen mole fraction.*

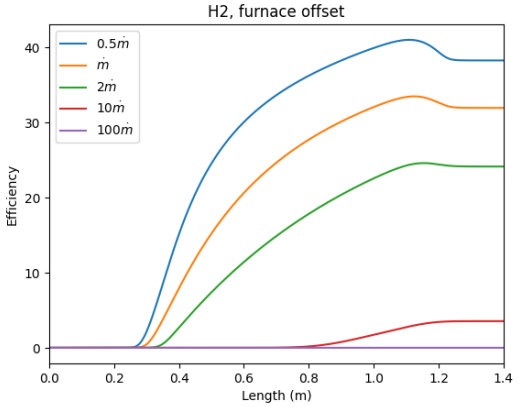

(d) *The hydrogen production efficiency.*

Figure 2: *The reservoir temperature profile, gas temperature profile, time step per unit length, H_2 mole fraction and production efficiency of the methane steam reforming reaction against the reactor length in meters, considering the temperature fit with parameters $A = 1140$, $a = 0.162$, $b = 1.254$, $B = 410$, and $E = 8.5$, for a set of multiples of Kahle et al.'s mass flow rate ($\dot{m}_{Kahle} = 2.74 \cdot 10^{-3}$ kg s^{-1}) [13], for a gas inside a one-dimensional plug-flow reactor.*

It can be observed from Figure 2a that when the mass flow rate of the gas increases, the gas temperature start to deviate more from the environment's temperature at each position within the reactor compared to lower mass flow rates. It can also be observed that for a mass flow rate of $\dot{m} = 10\dot{m}_{Kahle} = 2.74 \cdot 10^{-2}$ kg s^{-1} and $\dot{m} = 100\dot{m}_{Kahle} = 2.74 \cdot 10^{-1}$ kg s^{-1}, the maximum temperature of the gas does not meet the maximum temperature of the environment at any position within the reactor. In terms of the steepest temperature rise and fall, it seems that the temperature profile of the gas is shifted to the right for these mass flow rate compared to the temperature profile of the furnace itself.

It can be observed from Figure 2b that the time step at each position along the reactor's axis decreases with increasing mass flow rate. When comparing the observations of both Figure 2a and 2b with respect to the axial positions, it seems like there is a correlation between the temperature of the gas and the time step per unit length. A higher temperature seems to result in smaller time steps per unit length. This might be logical when considering Eq. 5 and Eq. 6 and corresponds with the expectations mentioned in the Methods section.

It can be observed from Figure 2c above that there is barely any hydrogen production for $z \leq 0.2$ m. Then for the majority of the mass flow rates (except the $10\dot{m}_{Kahle}$ and $100\dot{m}_{Kahle}$) the steepest hydrogen mole fraction increase occurs directly after this point before the mole fraction increase per unit length starts decreasing. Then for $z > 1.2$ m the hydrogen mole fraction becomes completely constant. For $\dot{m}_{Kahle} \leq \dot{m} < 10\dot{m}_{Kahle}$ it can be observed that the hydrogen mole fraction decreases before it becomes constant. For $\dot{m} = 10\dot{m}_{Kahle}$, the hydrogen mole fraction only starts increasing and becomes nonzero after a position between 0.6 m $< z <$ 0.8 m. Then for $z > 1.2$ m it becomes constant. When considering Figure 2a, it seems that these positions where the hydrogen mole fraction is constant and decreases correspond to the positions where the gas temperature is significantly lower than its maximum temperature. However, the hydrogen mole fraction produced for $\dot{m} = 10\dot{m}_{Kahle}$ is still nonzero even though the maximum gas temperature for this flow rate does not meet the maximum furnace temperature at any position in the reactor. As can be observed from 2d, the hydrogen production efficiency of the SMR reaction follows the same behavior.

The maximum realized hydrogen mole fraction decreases as the mass flow rate increases. The highest efficiency is therefore found for lower mass flow rates. This is in correspondence with the expectation stated in the Methods section that less reactions occur for higher mass flow rates due to lower residence times within the reactor.

6.3 Validation of the model

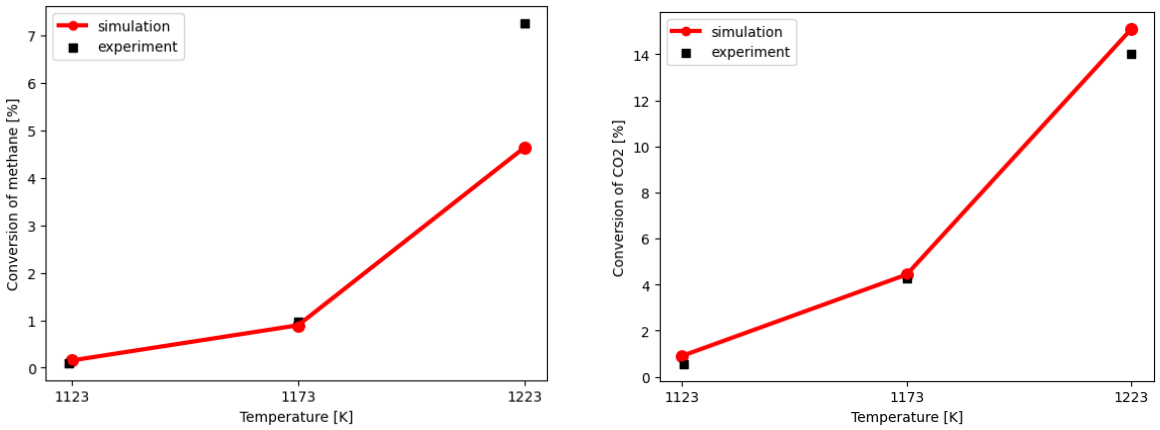

(a) Methane conversion

(b) CO_2 conversion

Figure 3: *The methane and CO_2 conversions for an initial gas composition of CO2:0.425, CH4:0.425, H2:0.1, Ar:0.05 against the temperature for both simulation and experimental data.*

From Figure 3 above it can be seen that the simulations used in this Thesis closely agrees with experimental data from Kahle et al. [13] for temperatures $\leq$ 1173 Kelvin. However, for higher temperatures, the results obtained from the simulations start to deviate more from the experimental data.

6.4 Limitations and improvements

Cantera's "gri30.yaml" might not take into account all possible reactions that are involved within a steam methane reactor [11]. For example, it does not take carbon sedimentation in the reactor into account. However, a test case had been performed using the kinetics package created by Dr. Anatoli V. Mokhov. This case simulated the hydrogen mole fraction but also the sedimentary carbon mole

fraction at chemical equilibrium. From this case it was observed that sedimentary carbon formation is not relevant when a methane-to-water mixing ratio of 1:2 is used (see Figure 4 in Appendix). However, if other reactions are missing, then the simulations could be improved by expanding the "gri30.yaml" reaction mechanism, or an entirely different reaction mechanism could be defined or used instead.

Already, heat transfer from a reservoir to the gas had been implemented to make the simulation more accurate to reality. However, only convective heat transfer between the reactor wall and the gas was considered. Moreover, the temperature of the environment outside was not considered either. Therefore, the model could be improved by implementing heat transfer between both the reservoir and the outside environment, as well between the outside environment and the gas if appropriate. When including heat exchange from the reservoir to an outside environment, the dimensions of the reservoir and a heat "producer" within the reservoir should be defined as well. Additionally, heat conduction through and radiative heat transfer from the reactor wall from the reservoir to the gas could be implemented next to convective heat transfer from the wall to the gas, effectively changing the overall heat coefficient used within cantera's wall object [11]. Convective heat transfer between reservoir and the reactor wall could be implemented as well to make the simulations more accurate.

The temperature profile used in this investigation was based on the fit to the temperature profile of Kahle et al. [13]. However only the upper bound of the fit was offset for it was assumed that this would result in a temperature profile that would correspond closer to reality. However, the slope of the increasing and decreasing parts of the profile might be inaccurate. Moreover, it was observed that the model used in this Thesis is less accurate compared to experimental values for temperatures above 1173 Kelvin as was stated earlier. Applying an offset to the temperature profile might therefore decreases the accuracy of the obtained results. However, from Figure 1 it can be observed that if this offset would not have been applied, that after 1000 seconds a hydrogen mole fraction less than 0.2 would have been realized. Thus applying an offset to the fit was assumed to be necessary.

6.5 Future research

For these simulations there was made use of a relative high reservoir temperature (almost 1600 K), for this resulted in the fastest reaction rate. However in practise this temperature will be less feasible due to heat transport from the reactor to the environment. This is probably why in practise there is often a catalyst incorporated in practical reactors. Implementing a catalyst could increase the reaction rate and hydrogen production efficiency at lower temperatures [14]. Future research could look into the temperature resulting in the maximum SMR hydrogen production efficiency for a variety of different catalysts.

The reactor by Kahle et al. operated using an internal pressure of 20 bar, while this investigation's simulations used an internal pressure of 1 atm [13]. Therefore, it could be interesting for future research to vary the pressure in addition to the temperature and mass flow rate and observe the change of the SMR hydrogen production efficiency of the same reactor as used in this investigation.

Additionally, the slope of the temperature profile fit could be increased and/or decreased to investigate its influence on the realized hydrogen mole fraction and the hydrogen production efficiency of the steam methane reforming reaction.

7 Conclusion

The research goal of this thesis was to examine the dependence of the SMR hydrogen production, in terms of the hydrogen mole fraction and production efficiency, on the mass flow rate of the gas in an ideal plug-flow reactor with an uneven temperature profile.

It was found that for a zero-dimensional reactor, which results were independent of mass flow rate, that the reaction rate increases for heightened temperatures. This effectively results in a higher hydrogen mole fraction after 1000 seconds because steady state was reached faster for higher temperatures.

For the plug-flow reactor, which essentially was a chain of zero-dimensional reactors, it was found that the deviation between the gas temperature and reservoir temperature increased with larger mass flow rates. The time step per unit length were found to decrease for increased mass flow rate. Both the lower overall temperature and decreased residence times resulted in the observed lower hydrogen mole fractions and lower production efficiency for higher mass flow rates.

It can thus be concluded that a higher reservoir temperature and a lower mass flow rate results in the highest obtainable efficiency for the temperatures and mass flow rates that have been evaluated for this Thesis.

Future research could look into the pressure dependence of the hydrogen production efficiency. The model could also be changed to incorporate a variety of catalysts to investigate the influence of a catalyst on the efficiency. Additionally, future research could also look into the efficiency dependence on the slope of the temperature fit. Moreover the model could be improved by implementing alternative forms of heat transfer, such as conductive and radiative heat transfer, as well heat transfer to an outside environment.

8 References

[1] Government-of-the-Netherlands, *Dutch vision on global climate action*, [Accessed 19. May. 2024]. [Online]. Available: https://www.government.nl/topics/climate-change/dutch-vision-on-global-climate-action.

[2] J. Moore and B. Shabani, "A critical study of stationary energy storage polices in australia in an international context: The role of hydrogen and battery technologies," *Energies*, vol. 9, p. 674, Aug. 2016. DOI: 10.3390/en9090674.

[3] Hydrogen-and-Fuel-Cell-Technologies-Office, *Fuel cells*, [Accessed 19. May. 2024]. [Online]. Available: https://www.energy.gov/eere/fuelcells/fuel-cells.

[4] Office-of-Fossil-Energy, *Hydrogen strategy enabling a low-carbon economy*.

[5] Hydrogen-and-Fuel-Cell-Technologies-Office, *Hydrogen production: Natural gas reforming*, [Accessed 19. May. 2024]. [Online]. Available: https://www.energy.gov/eere/fuelcells/hydrogen-production-natural-gas-reforming#:~:text=In%20steam%2Dmethane%20reforming%2C%20methane,for%20the%20reaction%20to%20proceed..

[6] E. U. Schlünder, I. C. for Heat, and M. Transfer., *Heat exchanger design handbook*. Hemisphere, 1983, ISBN: 3184190803.

[7] J. Warnatz, U. Maas, and R. W. Dibble, *Combustion : physical and chemical fundamentals, modeling and simulation, experiments, pollutant formation*, 4th. Springer, 2006.

[8] R. J. Kee, F. M. Rupley, E. Meeks, and J. A. Miller, *Chemkin-iii: A fortran chemical kinetics package for the analysis of gas-phase chemical and plasma kinetics*, 1996.

[9] R. J. Kee, M. E. Coltrin, P. Glarborg, and H. Zhu, "Low-dimensional reactors," in *Chemically Reacting Flow*. John Wiley Sons, Ltd, 2017, ch. 9, pp. 323–346, ISBN: 9781119186304. DOI: https://doi.org/10.1002/9781119186304.ch9. eprint: https://onlinelibrary.wiley.com/doi/pdf/10.1002/9781119186304.ch9. [Online]. Available: https://onlinelibrary.wiley.com/doi/abs/10.1002/9781119186304.ch9.

[10] J. H. Lienhard V and J. H. Lienhard IV, *A Heat Transfer Textbook*, 6th. Cambridge, MA: Phlogiston Press, Apr. 2024, 810 pp., Version 6.00. [Online]. Available: https://ahtt.mit.edu.

[11] D. G. Goodwin, H. K. Moffat, I. Schoegl, R. L. Speth, and B. W. Weber, *Cantera: An object-oriented software toolkit for chemical kinetics, thermodynamics, and transport processes*, https://www.cantera.org, Version 3.0.0, 2023. DOI: 10.5281/zenodo.8137090.

[12] G. P. Smith, D. M. Golden, M. Frenklach, *et al.*, *Gri-mech 3.0*, [Accessed: 29. June. 2024]. [Online]. Available: http://www.me.berkeley.edu/gri_mech/.

[13] L. C. Kahle, T. Roussière, L. Maier, *et al.*, "Methane dry reforming at high temperature and elevated pressure: Impact of gas-phase reactions," *Industrial and Engineering Chemistry Research*, vol. 52, pp. 11 920–11 930, 34 Aug. 2013, ISSN: 15205045. DOI: 10.1021/ie401048w.

[14] S. D. Angeli, G. Monteleone, A. Giaconia, and A. A. Lemonidou, "State-of-the-art catalysts for ch4 steam reforming at low temperature," *International Journal of Hydrogen Energy*, vol. 39, no. 5, pp. 1979–1997, 2014, ISSN: 0360-3199. DOI: https://doi.org/10.1016/j.ijhydene.2013.12.001. [Online]. Available: https://www.sciencedirect.com/science/article/pii/S0360319913028917.

9 Appendix

9.1 Additional graphs

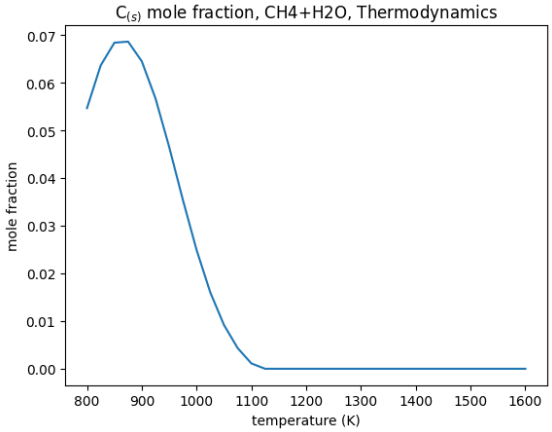

(a) Methane-to-water ratio 1:1

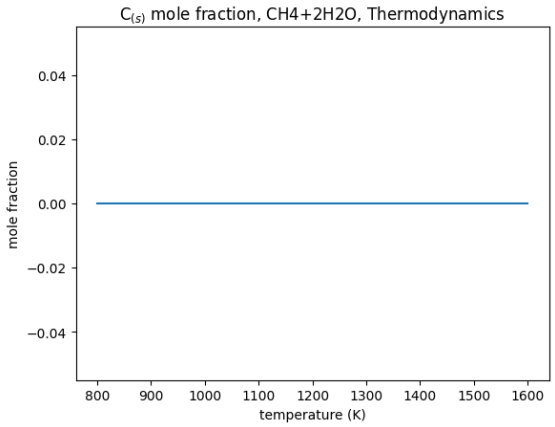

(b) Methane-to-water ratio 1:2

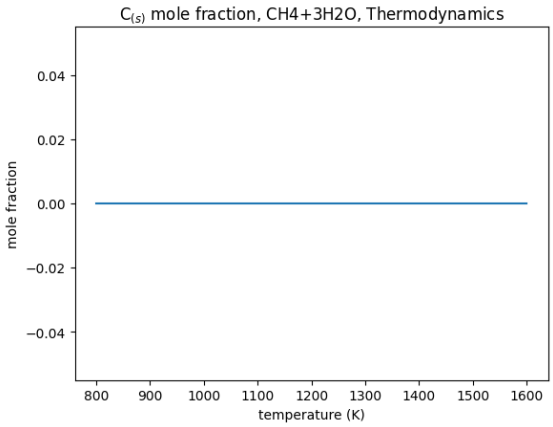

(c) Methane-to-water ratio 1:3

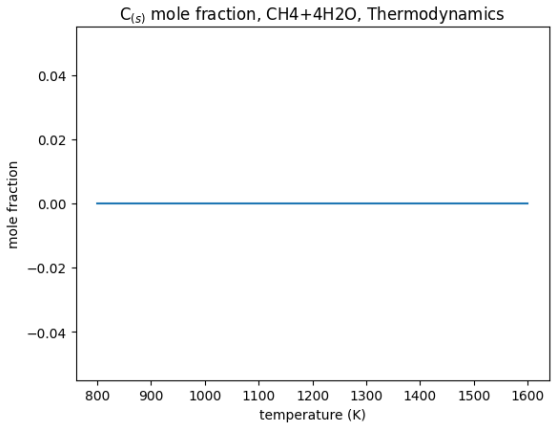

(d) Methane-to-water ratio 1:4

Figure 4: *The solid carbon deposition for different methane-to-water mixing ratios of 1:1, 1:2, 1:3, and 1:4 against the temperatures in Kelvin, considering the thermodynamic limit.*

From Figure 4 above it can be observed that only sedimentary carbon formation occurs for a methane-to-water ratio of 1:1.

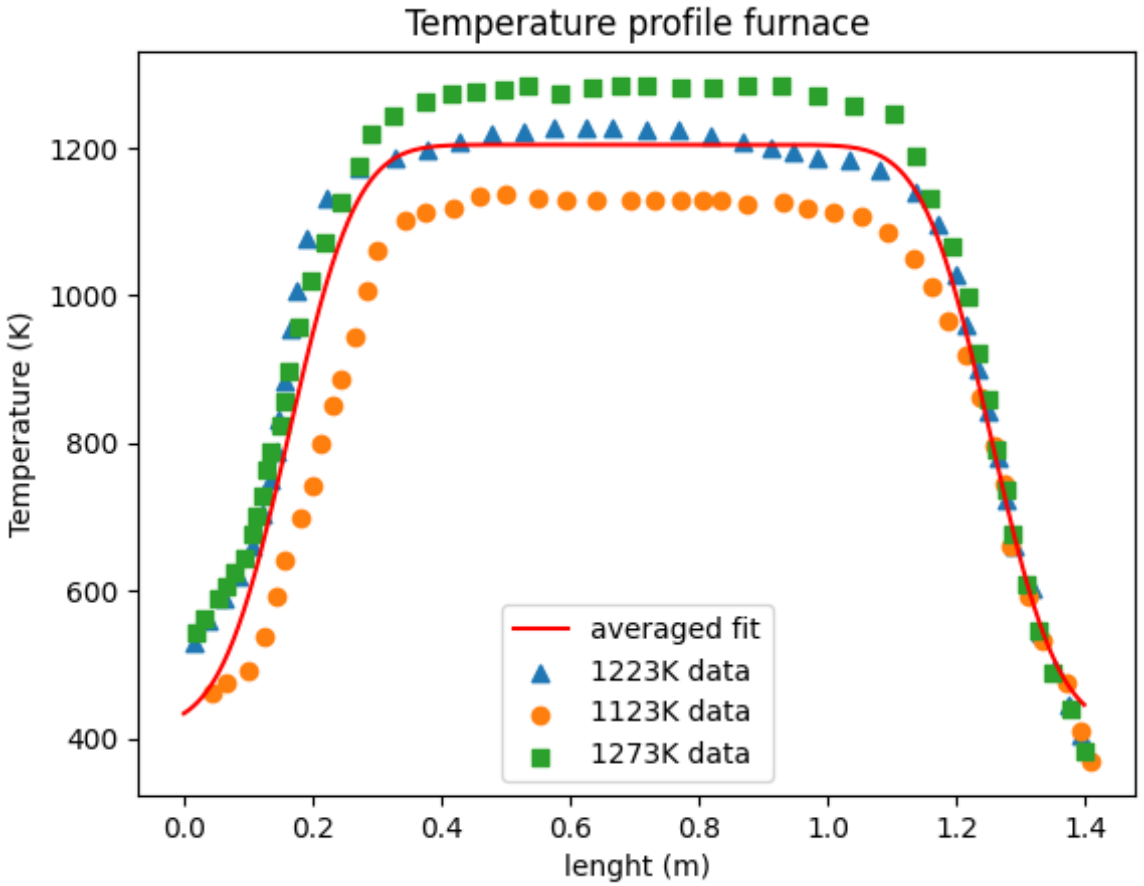

Figure 5: *The temperature profile data points of Kahle et al. [13] and the temperature fit made to the data with parameter* $A = 790 \pm 20$, $a = 0.162 \pm 0.003$, $b = 1.254 \pm 0.003$, $B = 410 \pm 20$, *and* $E = 8.5 \pm 0.4$, *against the length in meter.*

From Figure 5 above, it seems that the temperature profile as defined by Eq. 14 in the Methods section is appropriate to use as a fit to the data points of the three furnace temperature profiles of Kahle et al. [13].

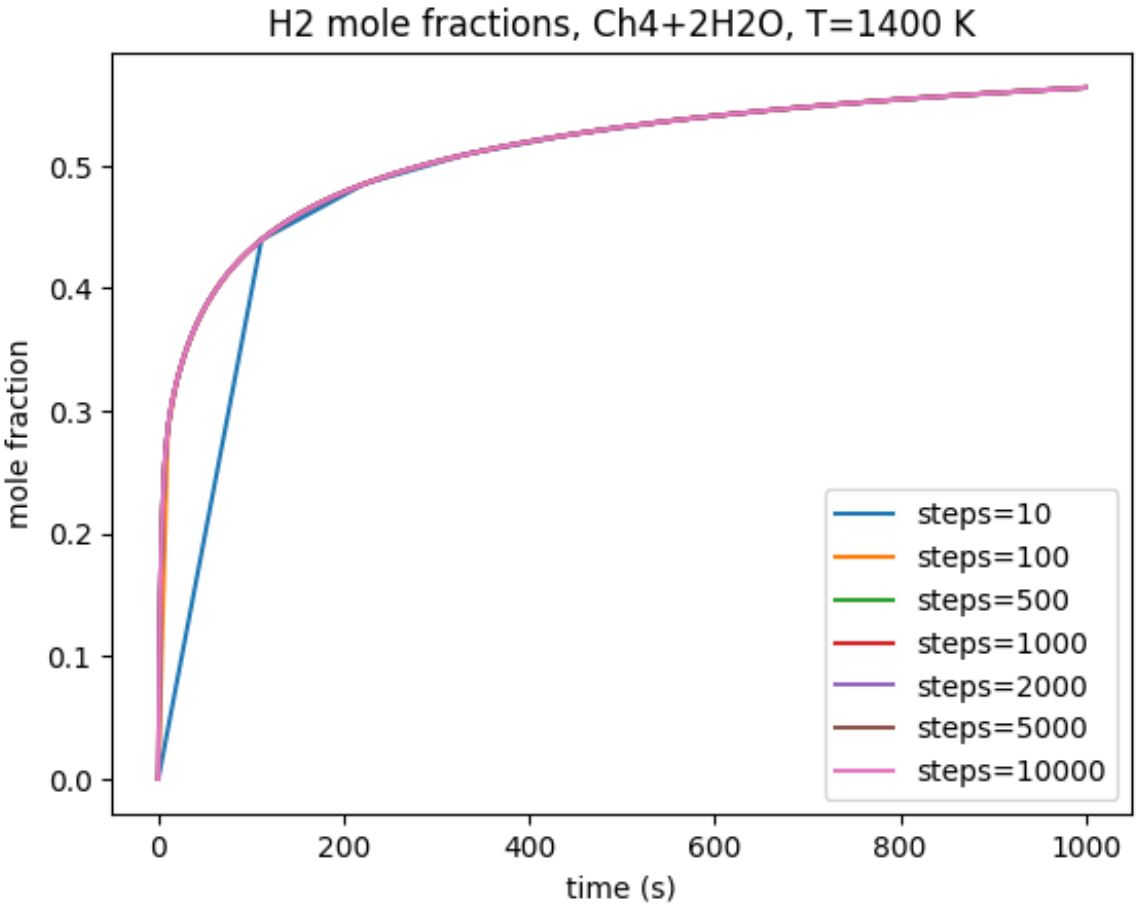

Figure 6: *The hydrogen mole fraction against the time in seconds at a temperature of 1400 Kelvin for a variety of iteration steps, for a gas inside a zero-dimensional reactor.*

From 6 above it can be observed that the differences in results almost can not be distinguished from the graph when the number of steps becomes larger than 2000.

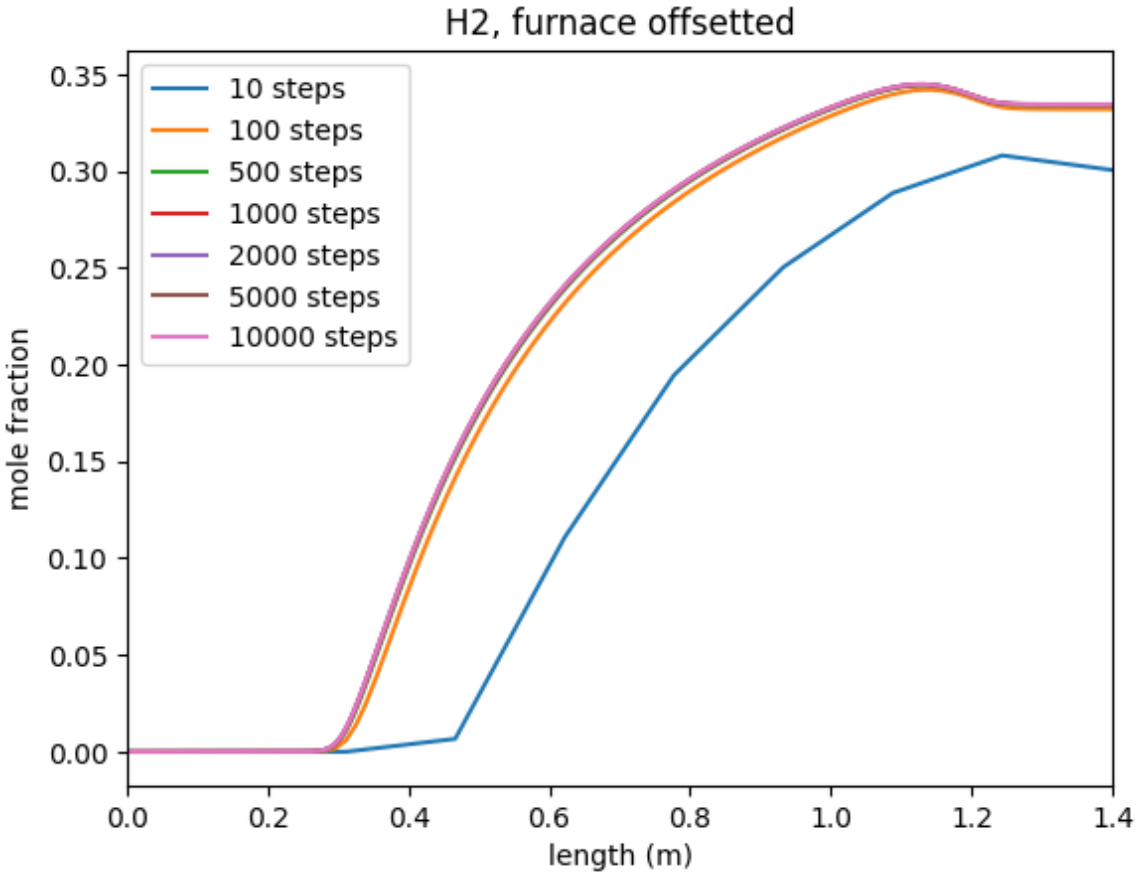

Figure 7: *The hydrogen mole fraction against the reactor length in meter for a variety of iteration steps, for a gas inside a one-dimensional plug-flow reactor.*

From 7 above it can be observed that the differences in results almost can not be distinguished from the graph when the number of steps becomes larger than 2000.